Electronic Supplementary Material (ESI) for Journal of Materials Chemistry C.

Supporting Information

Fabrication, Microstructural evolution and excellent EMW Absorbing Properties of SiC Fibers with High Iron Content

Shaohong Chen[a,b] †, *Xichao Dong*[a] †, *Xiaoji Yao*[a], *Pengfei Wu*[a], *Anhua Liu*[a,b] *, *Zhaoju Yu*[a] *

[a] Key Laboratory of High-Performance Ceramic Fibers of Ministry of Education, College of Materials (Xiamen University), Xiamen 361005, China

[b] Shenzhen Research Institute of Xiamen University, Shenzhen 518000, China

† These authors contributed equally to this work and should be considered co-first authors.

* Corresponding author's e-mail address: ahliu@xmu.edu.cn, zhaojuyu@xmu.edu.cn

Gel penetration chromatography (GPC) was used to test the *Mn* and PDI of PCS, VF-PCS-1, VF-PCS-2 and VF-PCS-3, and the results are shown in Fig. S1. The molecular weight and molecular weight distribution of PCS, VF-PCS-1, VF-PCS-2 and VF-PCS-3 show slight difference. This is because the hydrosilation reaction between Si-H and C=C has almost no influence on the molecular skeleton of PCS, leading to no obvious changes in the Mn and PDI distribution.

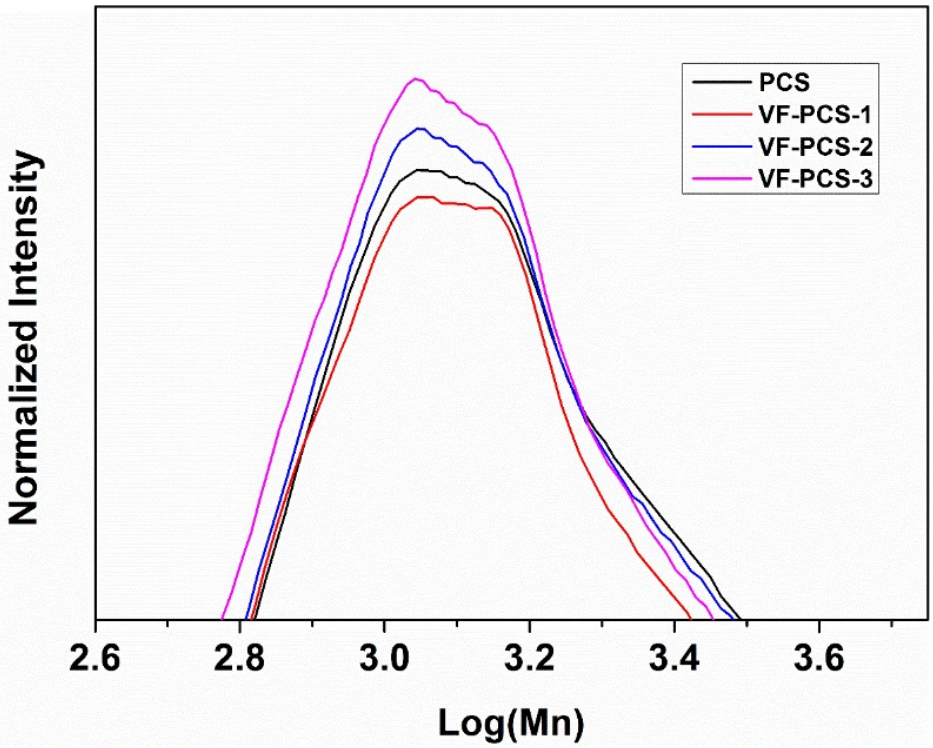

Fig. S1. GPC curves of PCS, VF-PCS-1, VF-PCS-2 and VF-PCS-3.

According to the literatures,[1, 2] PCS green fibers are normally cross-linked in the range of 150-200 °C for more than 10 h, and 8~12 wt% oxygen content is expected. In this paper, oxidation reactions between the oxygen in the hot air atmosphere and the active groups in the VF-PCSs were

used to achieve cross-linking of green fibers. After the cross-linking process, the insoluble part of the green fibers in THF is so called gel, which can quantitatively characterize the degree of cross-linking of the fibers. According to the literature survey,[3] the gel content of the green fiber should exceed 50%, and the fiber will not fuse in the subsequent pyrolysis process. As shown in Fig. S2, the gel content of cross-linked VF-PCS-1 fibers is higher than those of VF-PCS-2 and VF-PCS-3 when the oxidation temperature is lower than 240 °C. At lower oxidation temperature, the Si-H bonds are mainly involved to form Si-O-Si, and at a higher temperature, Si-CH_3 will also be oxidized to form Si-O-Si, making the gel content of the three fibers up to more than 90 %. It can also be seen from Fig. S2 that the gel content of VF-PCS-1, VF-PCS-2 and VF-PCS-3 all exceeds 50% when the crosslinking temperature is above 200 °C. Therefore, 200 °C was selected as the cross-linking temperature in the present work.

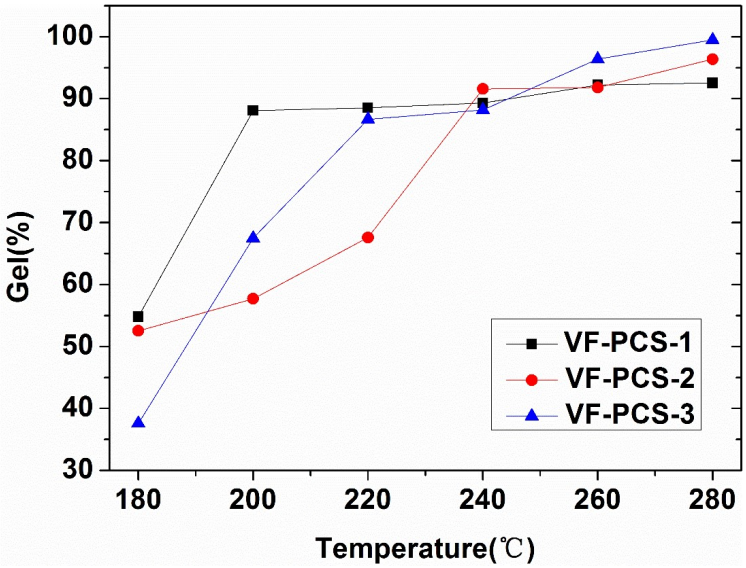

Fig. S2. Gel content of VF-PCS-1, VF-PCS-2 and VF-PCS-3 at different oxidation temperatures.

The SEM results (Fig. S3) show that the diameters of VF-PCS-1, VF-PCS-2 and VF-PCS-3 green fibers are about 25~30 μm, and the surfaces of fibers are smooth and compact.

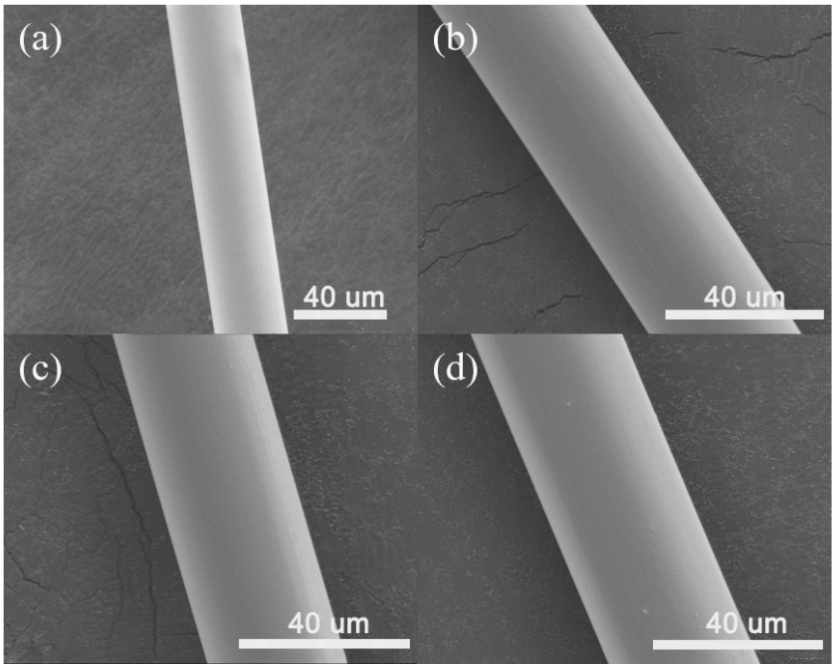

Fig. S3. SEM images of surface of green fibers (a) PCS, (b) VF-PCS-1, (c) VF-PCS-2 and (d) VF-PCS-3.

The FTIR was used to study the mechanism of cross-linking process, shown in Fig. S4. According to the literature,[4] Si-OH groups centered at 3680 cm^{-1} mainly originate from the oxidation of active Si-H bonds in PCS fibers, and C=O groups centered at 1710 cm^{-1} are due to the Si-CH_3 groups. During the cross-linking process, the PCS became cross-linked with the Si-O-Si bonds at 1080 cm^{-1} formed by a combination of the Si-OH groups. In Fig. S4, an absorption band at 1080 cm^{-1} is attributed to Si-O-Si groups, and the intensity of absorption peak of Si-OH decreases with the increase of Fe content in the feed. These results indicate that the oxidation

mechanism of VF-PCS-1, VF-PCS-2 and VF-PCS-3 is similar to that of PCS. After curing, Si-H was transformed to Si-O-Si and formed three-dimensional cross-linked network in the green fibers, so that the fibers did not fuse in the subsequent pyrolysis process.

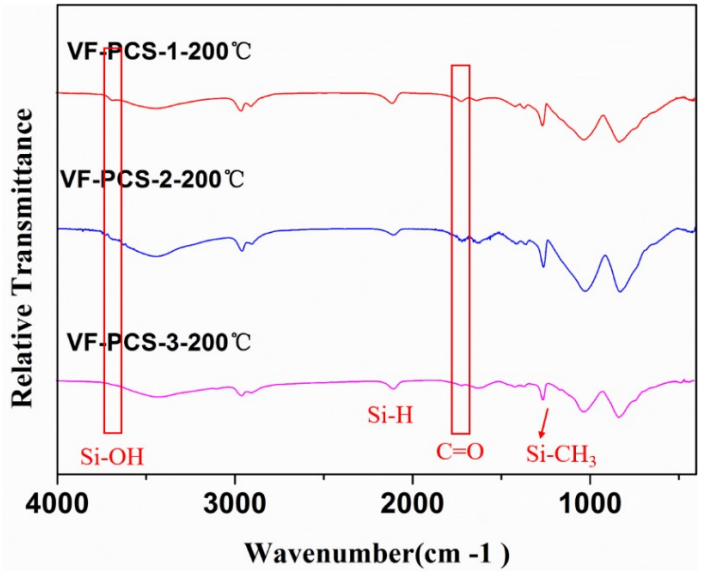

Fig. S4. FTIR spectra of cross-linked VF-PCS-1, VF-PCS-2 and VF-PCS-3 fibers at 200 °C.

The FTIR spectra of SiC fibers with different iron contents pyrolyzed at 900 and 1200 °C are shown in Fig. S5. It can be seen that the stretching vibration peaks of Si-H at 2100 cm^{-1}, the stretching vibration peaks of C-H at 2850 ~ 2980 cm^{-1} and the bending vibration peaks of C-H at 1250 cm^{-1} disappear after pyrolysis. In addition, overlapping peaks formed at 780, 800 ~ 1030 and 1100 cm^{-1}, which belong to the stretching vibration peaks of Si-C bonds and Si-O bonds in SiC and SiOC ceramics. With the increase of the amount of Fe, the intensity and the position of vibration peaks Si-C and Si-O bonds in ceramic fibers are almost the same. The FTIR results indicate that the structure of ceramic fibers didn't change with the increase of the amount of Fe, and the main components in ceramic fibers are still SiC and SiOC.

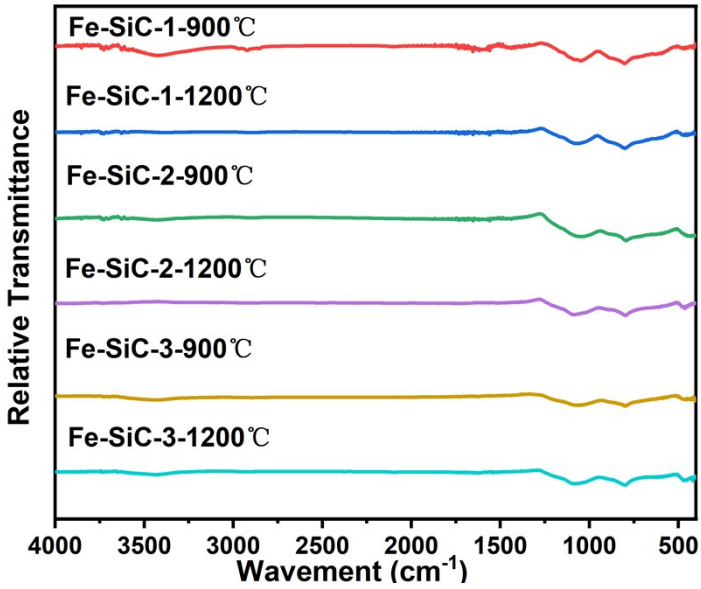

Fig. S5. FTIR spectra of Fe-SiC fibers.

Magnetic properties of Fe-SiC-1, Fe-SiC-2 and Fe-SiC-3 fibers were investigated and the results are shown in Fig. S6. In general, the saturated magnetization and coercivity of Fe-SiC fibers increase with the increase of Fe content. After pyrolysis at 900 °C, the saturated magnetization and coercivity of Fe-SiC-3 fibers are about 6.8 emu/g and 19.17 Oe, respectively. This is because the Fe_5Si_3 are ferromagnetic compounds, and the magnetic properties are enhanced with the increase of Fe content. At the same time, with the increase of pyrolysis temperature, the saturation magnetization and coercivity also increase. After heat-treatment at 1200 °C, the saturation magnetization and coercivity of Fe-SiC-3 are 8.14 emu/g and 89.25 Oe, respectively, indicating that the saturation magnetization and coercivity also increase with the increase of annealing temperatures. This is because at 1200 °C, Fe_5Si_3 is transformed into Fe_3Si and the grain size also increases. With the increase of magnetic properties, the magnetic loss capacity will be strengthened, which will have a positive effect on the EMW absorption performance of the fiber.

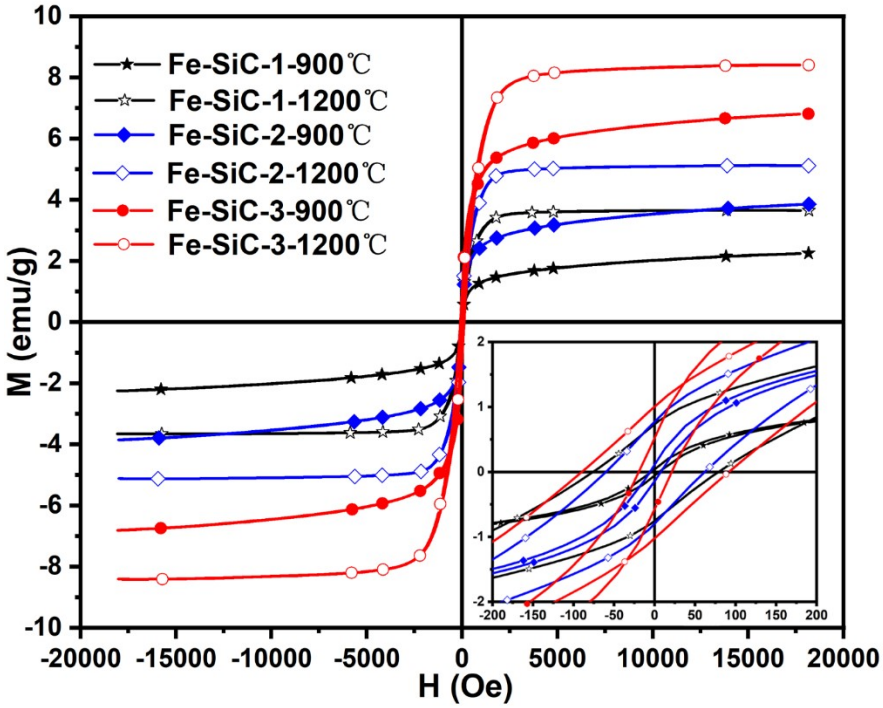

Fig. S6. Magnetic properties of Fe-SiC-1, Fe-SiC-2 and Fe-SiC-3 fibers.

Dielectric loss and magnetic loss are the main attenuation modes of EMW. In the range of gigagertz (GHz), polarization loss (interface polarization and dipole polarization) and conduction loss are the main modes of dielectric loss,[5, 6] while the eddy current effect and ferromagnetic resonance play important roles in magnetic loss.[7, 8] The relative complex permittivity ($\varepsilon_r = \varepsilon' - j\varepsilon''$) and relative complex permeability ($\mu_r = \mu' - j\mu''$) were measured by the coaxial transmission/reflection method in the X-band to investigate the dielectric loss and magnetic loss capacity of Fe-SiC fibers. As shown in Fig. S7(a), with increasing either Fe content or annealing temperature, the ε' value of the dielectric constant increases. The ε' value represents the energy

storage capacity. However, the greater the ε' value is, the greater the reflection of the absorbing material to the electromagnetic wave will be. Fig. S7(b) shows that the ε" decreases either with the increase of Fe content or with the annealing temperature. The ε" value is related to the dielectric loss, which means that with the increase of Fe content or annealing temperature, the dielectric loss capacity of the fiber becomes weaker. Besides, the loss tangent $\tan\delta_\varepsilon$ ($\tan\delta_\varepsilon = \varepsilon''/\varepsilon'$) of dielectric materials is frequently used to describe the dielectric properties. As shown in Fig. S7(e), the $\tan\delta_\varepsilon$ is in the range of 0.05-0.2, which indicates promising EMW absorbing properties.

Figs. S7(c), S7(d) and 7S(f) show real permeability (μ'), imaginary permeability (μ") and tangent loss (tanδμ) of Fe-SiC fibers. It can be observed that the μ', μ" and the tanδμ all increase with the increase of annealing temperature and Fe content. This is consistent with the increase of the saturation magnetization and coercivity of the fibers, as shown in Fig.S6. It indicates that the magnetic loss ability of materials can be improved by increasing the magnetic property of materials. According to the loss mechanism, absorbing materials can be divided into dielectric loss absorbing type and magnetic loss absorbing type, which exhibit absorbing effect on high/low frequency radar waves, respectively. In the present work, our SiC-Fe fibers exhibit both dielectric and magnetic loss capacity, which are expected to improve their final EMW performance.

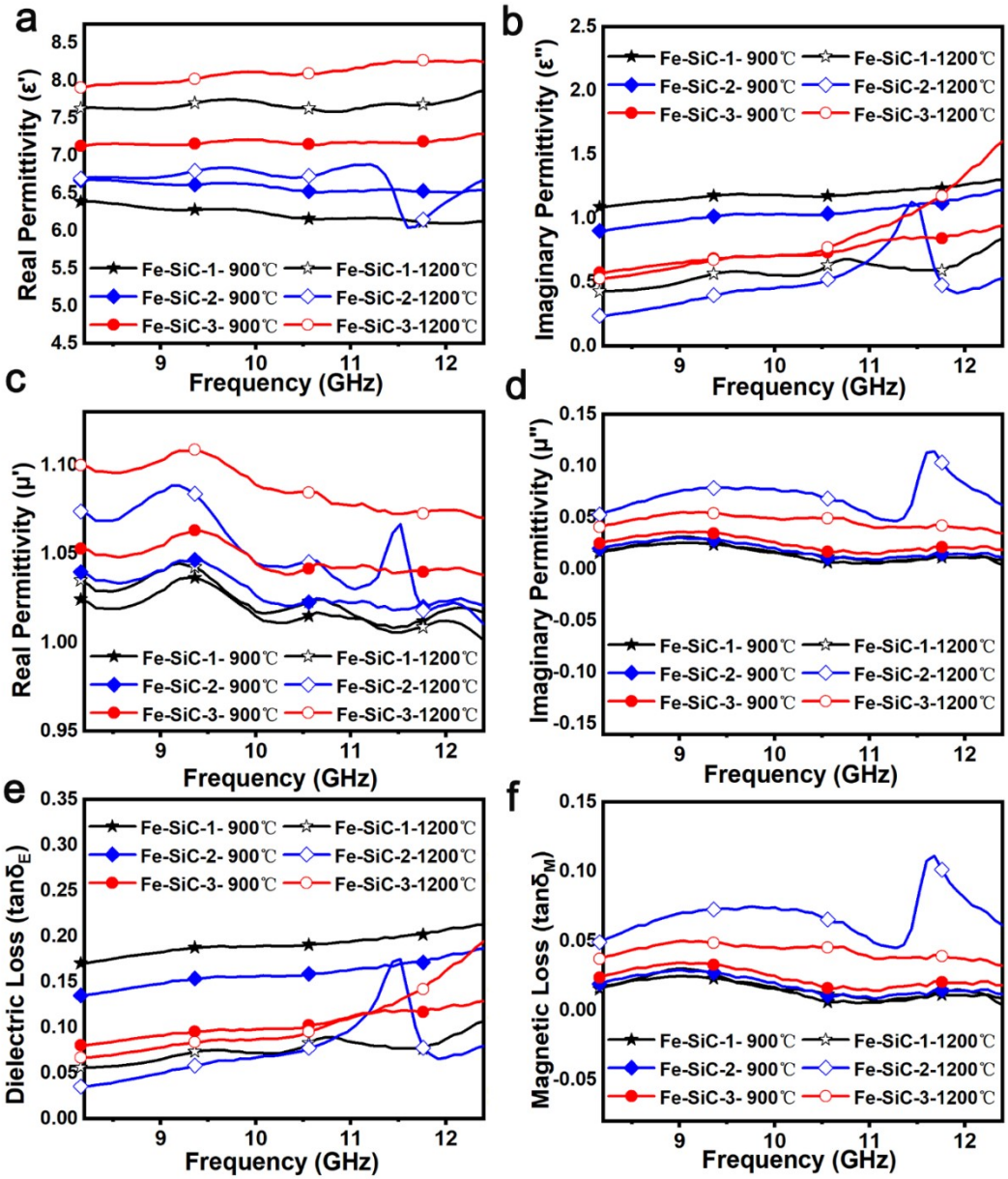

Fig. S7. (a) The real permittivity (ε'), (b) imaginary permittivity (ε"), (c) real permeability (μ'), (d) imaginary permeability (μ"), (e) tangent loss (tan δε) and (f) tangent loss (tan δμ) of Fe-SiC fibers.

As shown in Fig. S8, the EMW absorbing capacity of Fe-SiC fibers with different Fe content and pyrolysis temperatures was analyzed in detail. In general, all the SiC-Fe fibers show good EMW performance since the RL_{min} is lower than -10 dB by tuning the thickness.

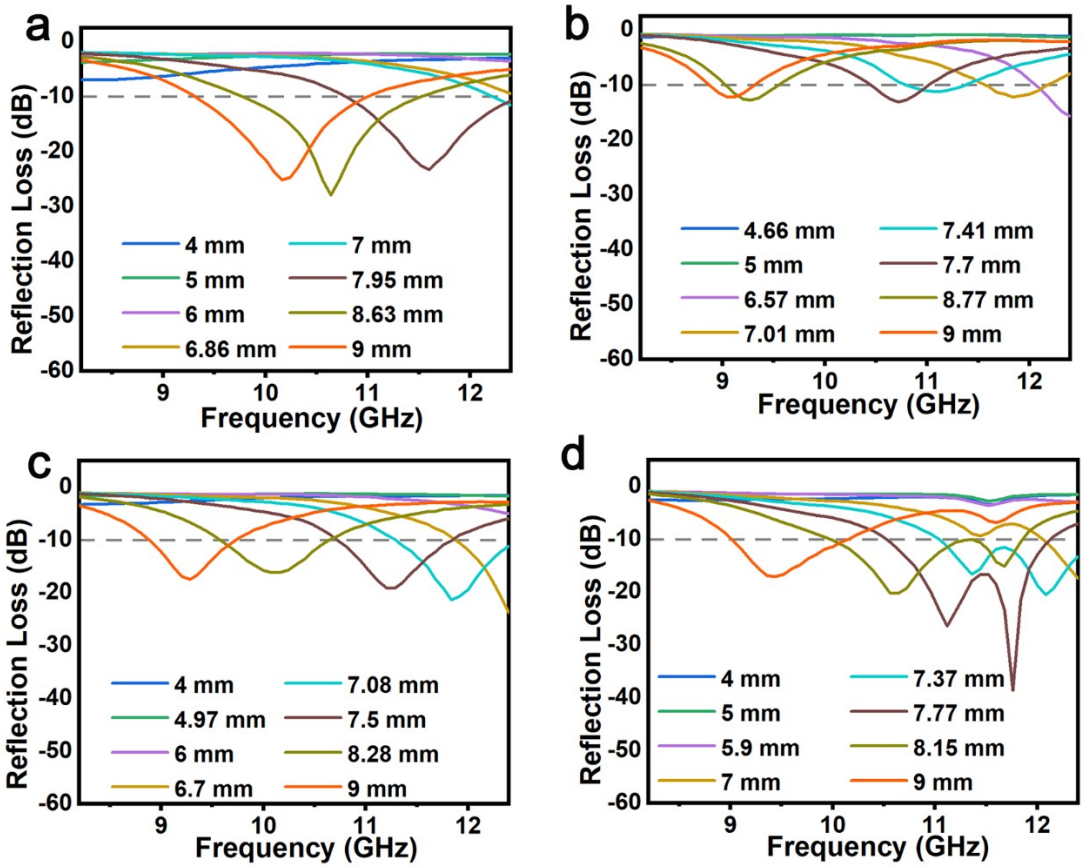

Fig. S8. EMW absorption performance in the X-band of (a) Fe-SiC-1-900 °C, (b) Fe-SiC-1-1200 °C, (c) Fe-SiC-2-1200 °C and (d) Fe-SiC-3-900 °C.

References:

1. A. Liu, J. Chen, S. Ding, Y. Yao, L. Liu, F. Li and L. Chen, *J. Mater. Chem. C*, 2014, **2**, 4980-4988.
2. K. Okamura, M. Sato and Y. Hasegawa, *Journal of Materials Science Letters*, 1983, **2**, 769-771.
3. H. Ichikawa, F. Machino, S. Mitsuno, T. Ishikawa, K. Okamura and Y. Hasegawa, *Journal of Materials Science*, 1986, **21**, 4352-4358.
4. Y. Hasegawa, M. Iimura and S. Yajima, *Journal of Materials Science*, 1980, **15**, 720-728.
5. H. Yang, M. Cao, Y. Li, H. Shi, Z. Hou, X. Fang, H. Jin, W. Wang and J. Yuan, *Advanced Optical Materials*, 2014, **2**, 214-219.
6. X. Liang, B. Quan, G. Ji, W. Liu, Y. Cheng, B. Zhang and Y. Du, *Inorganic Chemistry Frontiers*, 2016, **3**, 1516-1526.
7. B. Lu, X. L. Dong, H. Huang, X. F. Zhang, X. G. Zhu, J. P. Lei and J. P. Sun, *Journal of Magnetism and Magnetic Materials*, 2008, **320**, 1106-1111.
8. M. Z. Wu, Y. D. Zhang, S. Hui, T. D. Xiao, S. H. Ge, W. A. Hines, J. I. Budnick and G. W. Taylor, *Applied Physics Letters*, 2002, **80**, 4404-4406.